0273-2289/87/1401-0001$04.00

A Photosynthetic Photoelectrochemical Cell Using Phenazine Methosulfate and Phenazine Ethosulfate as Electron Acceptors

DOUGLAS G. SANDERSON,[1] ELIZABETH L. GROSS,[1] AND MICHAEL SEIBERT*,[2]

[1]Departments of Chemistry and Biochemistry, The Ohio State University, Columbus, OH, 43210; and [2]Solar Energy Research Institute, Golden, CO, 80401 (A Division of the Midwest Research Institute. Operated for the US Department of Energy under Contract # DE-AC-02-83 CH 10093)

Received October 18, 1985; Accepted July 14, 1986

ABSTRACT

Several recent studies have demonstrated that photosystem I (PSI), one of the two light-active complexes of photosynthesis, can be used as a light transducer in a biological photoelectrochemical cell. This paper examines the results of using phenazine methosulfate (PMS) and phenazine ethosulfate (PES) as an electron acceptor in such a cell. The PMS and PES have relatively high formal potentials compared to flavin mononucleotide (FMN) and other acceptors used in the past, yet the PMS and PES resulted in power outputs and conversion efficiencies second only to the use of FMN as an acceptor. The mechanism of action has been interpreted in terms of electroactive products of parent compounds formed during the normal function of the cell under illuminated conditions. For example, photolysis and cyclic voltammetry data demonstrate that pyocyanin (Py) [formal potential = −0.37 vs saturated calomel electrode (SCE) at pH 8.5], the photoproduct of PMS, is the electroactive species in cells containing PMS (formal potential = −0.19 vs SCE at pH 8.5). Similar phenomena were observed for PES and FMN. The power output of the cell

*Author to whom all correspondence and reprint requests should be addressed.

results from about equal contributions from a cyclic photosynthetic component and a component caused by the direct photoreduction of the acceptor and reoxidation by sacrificial donors in the buffer. Future research directions are discussed in terms of designing cells that function purely in the photosynthetic or photochemical modes.

Index Entries: Photoelectrochemical cell; photosystem I, photosynthesis; photochemistry; acceptors; phenazine methosulfate; phenazine ethosulfate; flavin mononucleotide; pyocyanin; electrochemistry; solar cell.

INTRODUCTION

Bhardwaj et al. (*1–3*) have reported on the development of a photoelectrochemical cell that can utilize the energy inherent in the light-induced separation of charge within the reaction center of photosystem I (PSI) particles as a driving force. In this device, a membrane containing PSI particles isolated from spinach separates two compartments that contain solutions of a PSI electron acceptor and electron donor, respectively. Irradiation of the PSI particles produces a strong reductant [P430, $E^{\circ\prime}$ (formal potential vs NHE {normal hydrogen electron}, −0.42 V at pH 7) = −0.5 V] and a weak oxidant ($P700^+$, $E^{\circ\prime}$ = +0.43 V) that can interact with the electron acceptor and donor to produce a gradient of chemical potential (*4*). Electrodes in each compartment connect the cell, which acts like a battery in the light, to an external circuit. This "uphill" transport of electrons results in the reduction of an electron acceptor in one compartment and the oxidation of an electron donor in the other. The standard free energy change [$\Delta G^{\circ\prime}$ (at pH 7)] for the photosynthetic contribution can be determined from:

$$\Delta G^{\circ\prime} = -nF(E^{\circ\prime}_{acc} - E^{\circ\prime}_{don}) \quad (1)$$

where n is the number of electrons transferred, F is the Faraday constant, $E^{\circ\prime}_{acc}$ is the formal potential of the acceptor at pH 7, and $E^{\circ\prime}_{don}$ is the formal potential of the donor also at pH 7.

Several recent papers have described the operation of this "biological solar cell," using various photoreducible dyes, including flavin mononucleotide (FMN) (*1–3,5,6*), phenosafranine (PS) (*7*), methylviologen (MV) (*8*), and anthroquinone-2-sulfonate (AQS) (*3,5*) as electron acceptors. The redox potentials of these acceptors are quite negative (FMN, $E^{\circ\prime}$ = −0.19 V; PS, $E^{\circ\prime}$ = −0.25 V; MV, $E^{\circ\prime}$ = −0.44 V; and AQS, $E^{\circ\prime}$ = −0.18 V) relative to the electron donors used: $Fe(CN)^{-4}_{6}$ (*1–3,5*), $E^{\circ\prime}$ = +0.42 V; diaminodurene (DAD) (*4*), $E^{\circ\prime}$ = +0.22 V; and *N,N,N′,N′*-tetramethylphenylenediamine (TMPD) (*4*), $E^{\circ\prime}$ = +0.26 V. The action spectrum of the cell output indicates that, in fact, two reactions (Fig. 1) contribute to the photovoltages and photocurrents generated by the cell (*5*). The first, as mentioned above, is the photosynthetic reduction of a PSI electron acceptor, such as FMN, and the oxidation of a PSI electron

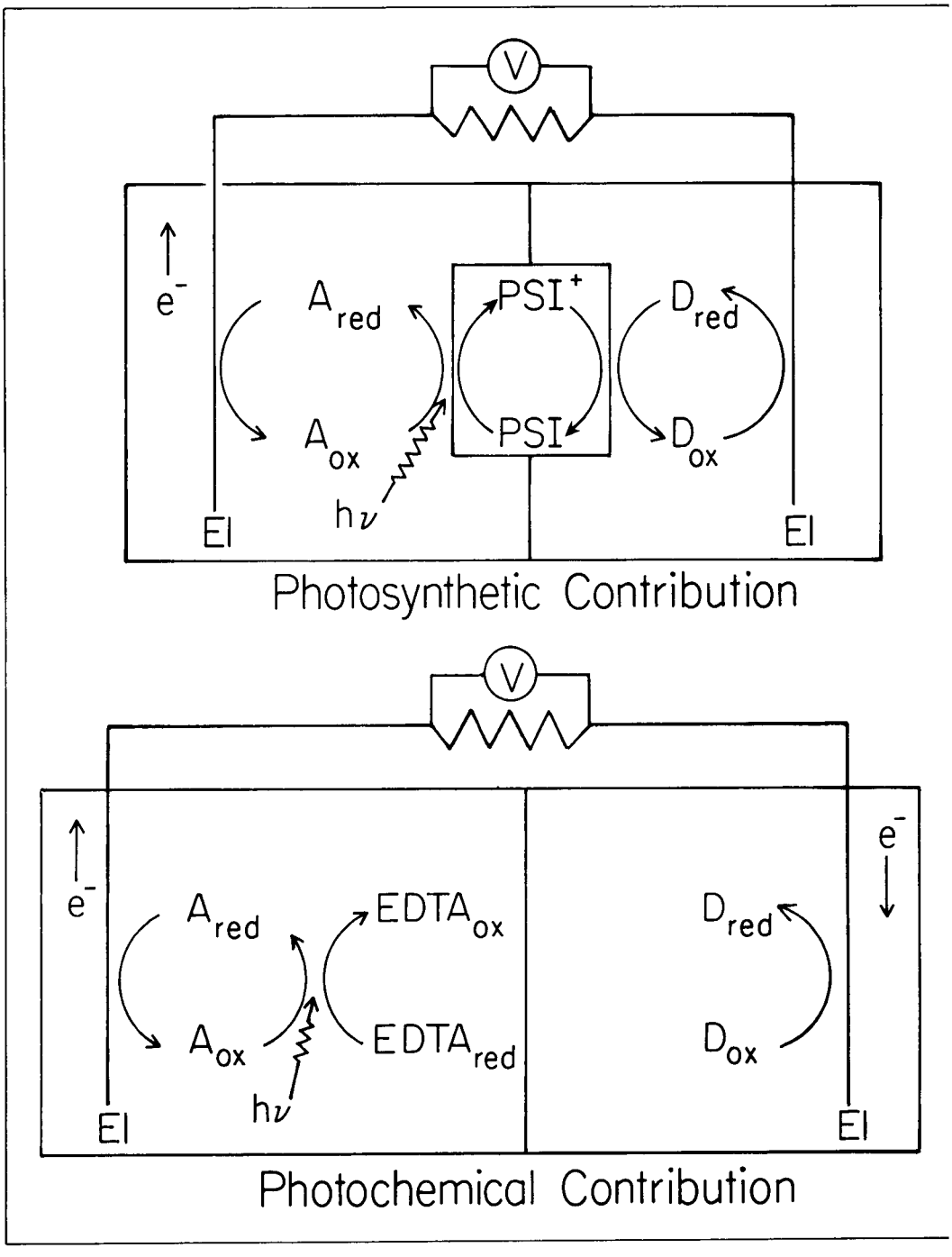

Fig. 1. The two mechanisms of photopotential and photocurrent generation. D_{ox} and D_{red} represent the oxidized [Fe(CN) $_6^{3}$] and reduced [Fe(CN) $_6^{4}$] forms of the electron donor, respectively. A_{ox} and A_{red} are the oxidized and reduced forms of the electron acceptor. El represents the RVC electrodes.

donor, such as $K_4Fe(CN)_6$. The reaction, mediated by PSI, goes as follows:

$$2H^+ + FMN + 2Fe(CN)_6^{-4} \xrightarrow{h\nu,\ PSI} FMNH_2 + 2Fe(CN)_6^{-3} \quad (2)$$

The second reaction is the direct photoreduction of the acceptor at the expense of sacrificial donors, such as EDTA, Tris-HCl, or Tricine buffers. It does not require the light reaction associated with PSI, *per se*, and goes as follows:

$$FMN + EDTA_{red} + H_2O \xrightarrow{h\nu} FMNH_2 + \text{oxidation products} \quad (3)$$

Although the actual power of the cell should depend on Eq. (1), a number of other factors may also be involved. These include the efficiency of the photosynthetic processes, the efficiencies of the reduction and oxidation of the dyes by PSI, the efficiency of the direct photoreduction of the acceptor dye, the rates of diffusion of the electroactive species to the electrodes, and the rates of reaction of the electroreactive species at the electrode surfaces. With this in mind, the best results obtained so far with this type of cell were achieved when FMN was used as the electron acceptor, when $K_3Fe(CN)_6/K_4Fe(CN)_6$ was used as the electron donor, and when the cell electrodes were made from reticulated vitreous carbon (RVC) (*9*). These conditions resulted in a maximum power output of 2180 μW (272 μW/cm) and a power conversion efficiency of 3.9%. The efficiency figure, of course, ignores the sacrificial nature of the photochemical contribution.

In this paper, we report in particular on the use of phenazine methosulfate (PMS) and phenazine ethosulfate (PES) as electron acceptors and explore the effects of their electrochemical and photochemical properties on cell function. Of interest in the above context are their significantly more positive formal potentials (PMS, $E^{\circ\prime} = 0.076$V; PES, $E^{\circ\prime} = 0.068$) compared to the other electron acceptors that have been used previously. Despite this fact, however, both afford power outputs and conversion efficiencies superior to all other acceptors tested, except for FMN (*9*).

MATERIALS AND METHODS

Measurement of Photovoltages

The cell experimental design and photoresponse measurements were the same as described previously (*5*), except when noted otherwise. The PSI particles were isolated according to the method of Shiozawa et al. (*10*), as modified by Gross and Grenier (*11*). The PSI particles containing 80 μg of chlorophyll, as measured by the method of Arnon (*12*), were aspirated onto a Metricel (cellulose triacetate) filter, with an area of 1 cm^2 and a pore size of 0.45 μm. The PSI-containing filter was placed

between two aqueous compartments in the cell. Each compartment contained 32 mL of a solution composed of 160 m*M* Tris-HCl (at indicated pH). In addition, the acceptor compartment contained 3 m*M* PMS (or PES) and 5 m*M* EDTA, whereas the donor compartment contained a mixture of 5.25 m*M* $K_3Fe(CN)_6$ and 1.75 m*M* $K_4Fe(CN)_6$. The $Fe(CN)_6^{-3}/Fe(CN)_6^{4}$ mixture was necessary to poise the donor compartment at the correct redox potential for maximal cell response (*5*). The acceptor side of the cell was illuminated with white tungsten light (I = 1970 W/m^2) from a slide projector. An 8 cm^2 area of acceptor solution (path length, 3 cm) and a 1 cm^2 area of PSI were illuminated. Anaerobicity was maintained by bubbling argon through both compartments of the cell. Each compartment contained an RVC (100S mesh) electrode with an area of 35 cm^2. The measured areas of the RVC electrodes were corrected for thickness, i.e., the areas of the sides were included. Electrical contact between the electrode and the external circuit was made with a platinum wire.

Photovoltages were measured across a variable load resistance box, using a Radiometer Model 26 pH meter as a high-impedence voltmeter. Light intensities were measured using a Yellow Springs Instruments Model 65 Radiometer. The photochemical contribution was determined after inactivating the PSI particles on the filter with 15% trichloroacetic acid (TCA). Cyclic voltammetry was performed with a Bioanalytical Systems Model CV-1B voltammetry module and recorded on a Houston Instruments Series 100 X–Y recorder. The working electrode used was carbon paste, the counter electrode was a platinum wire, and the reference electrode was a saturated calomel electrode (SCE). Absorption spectra were obtained on a Cary Model 118-C spectrophotometer.

Reticulated vitreous carbon was obtained from Fluorocarbon Process Systems Division, Anaheim, CA and had a porosity of 100 pores/linear inch. The PMS and PES were obtained from Sigma Chemical Company, St. Louis, MO. Silia gel 60 (70–230 mesh) and aluminum TLC sheets, precoated with silica gel F-254, were obtained from E & M Laboratories, Darmstadt, Germany. All other chemicals were of reagent grade.

Synthesis and Purification of Pyocyanin

Pyocyanin (Py) was prepared by photochemical oxidation of PMS in aqueous solution (*13*). Approximately 12 mL of a 3–4 mg/mL solution of PMS in 0.01*M* Tris-HCl (pH 7.0) was photolyzed for 40 min in tungsten light illuminated through a blue, low-pass, optical filter (<456 nm). The resulting blue–green solution was lyophilized and the residue dissolved in 2 mL of methanol. This solution was then adsorbed onto a silica gel 60 column (2.5 × 40 cm) that had previously been equilibrated with 1% methanol in chloroform. Elution was accomplished with 15% methanol in chloroform, and the products appeared in the following order: A yellow-colored side product, an orange-colored side product, and,

finally, the blue-colored Py mixture. A yellow–green material remained absorbed on the packing gel. Solvent was removed from each of these three solutions by rotary evaporation. Photolysis with white light produced the same products, but with somewhat different relative yields.

Further purification of Py was performed by redissolving the resulting blue residue in about 2 mL of methanol and adsorbing it onto a second column (2.5 × 26 cm) packed with silica gel 60 and equilibrated with 1% methanol in chloroform. From this material a yellow impurity was eluted with 1% methanol in chloroform, a red impurity with 6% MeOH in $CHCl_3$, and pure, blue Py with 15% MeOH in $CHCl_3$. The solvent was removed from this solution by rotary evaporation.

Thin-layer chromatography on aluminum sheets precoated with silica gel F-254 was performed on the products obtained from the second column. R_f values for the blue (Py), red, and yellow products were 0.62, 0.82, and 0.89, respectively, in 1:1 methanol–chloroform (solvent system A) and 0.37, 0.81, and 0.79, respectively, in 3:2:1 ethyl acetate–acetic acid–water (solvent system B). Absorption spectra in chloroform showed the following maxima: blue (Py) 740, 699, 327, 310, 255, and 243 nm; red 517, 364, 350, 289, 281, and 252 nm; and yellow 653, 600, 370, 364, and 363 nm. The Py was crystallized from chloroform and exhibited a melting point of 130–131° C. These data obtained for Py are in good agreement with the literature accepted values (*14–17*).

RESULTS

The effect of pH and acceptor concentrations on the power output of the solar cell are shown in Fig. 2. The power is maximal at pH 8.2 for both PMS and PES. In both cases the power output increases with increasing acceptor concentration, reaching a maximum between 0.5 and 0.6 m*M* and decreasing slightly at higher concentrations.

Table 1 summarizes the electrochemical results obtained from the use of PMS and PES as electron acceptors from PSI in the cell. Also shown for comparison are the results obtained using FMN, the most efficient acceptor found to date. The open circuit voltages produced by PMS and PES in the cell are lower than those observed for FMN. This is consistent with the more positive formal potentials for PMS and PES. The photopotentials are also comparable to those obtained using the electron acceptors listed in the Introduction (*1–3, 5–9*). However, PES and PMS, respectively, afford power outputs and power conversion efficiencies (ignoring the sacrificial nature of the photochemical component) second only to the use of FMN as the acceptor. This is an unexpected observation in light of the rather positive formal potentials of PMS, PES, and, in fact, FMN relative to other acceptors that have been used (1–3, 5–9). Some interesting insights into this anomaly are found upon examination of the photochemical reactions involving PMS, PES, and FMN.

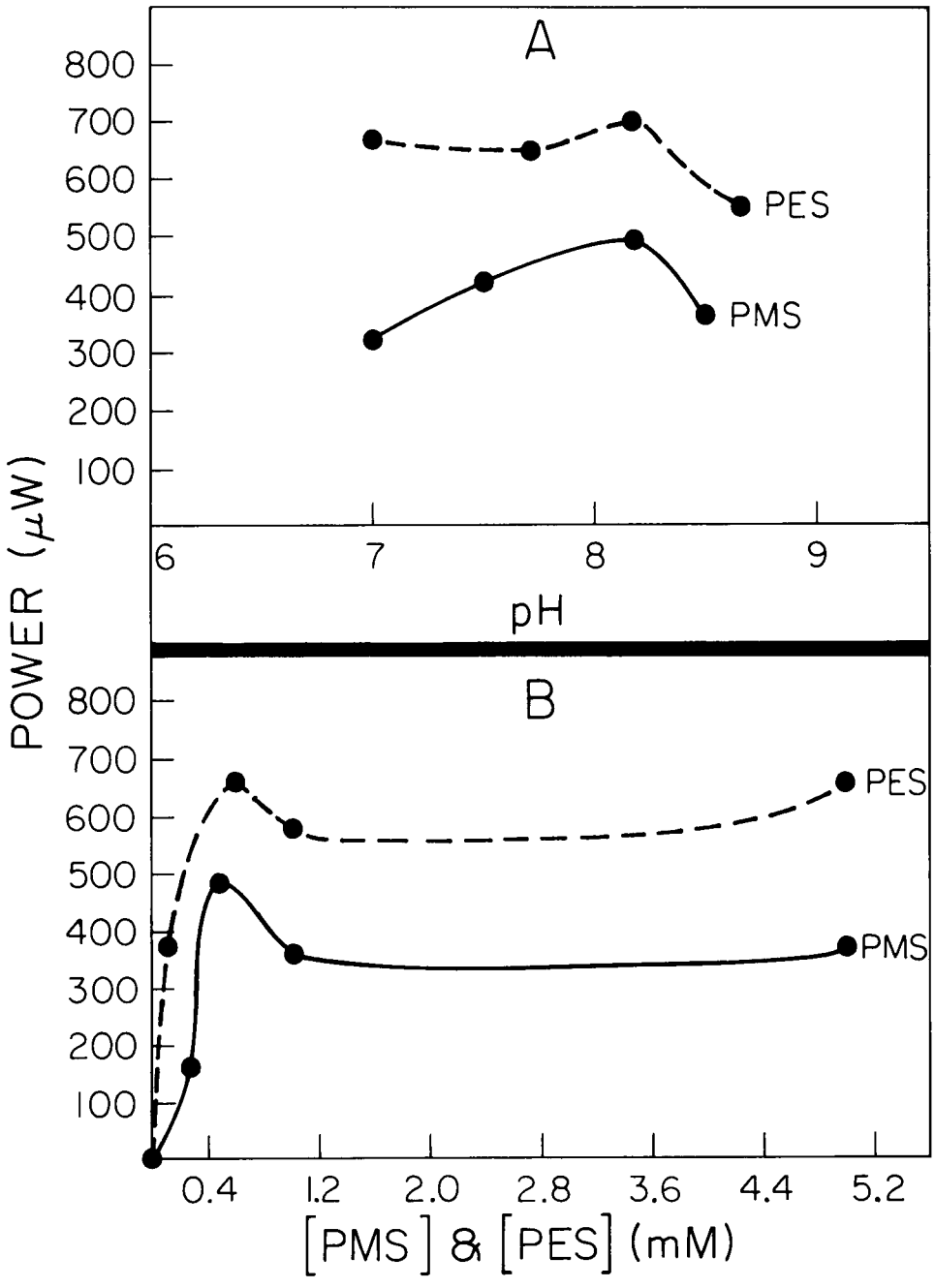

Fig. 2. (A) The effect of pH on power output. [PMS] = [PES] = 0.5 m*M* in 160 m*M* Tris-HCl buffer at the indicated pH. Other conditions were as described in the Materials and Methods section. (B) The effect of varying the PMS and PES concentration on the power output. The PMS and PES were dissolved in 160 m*M* Tris-HCl (pH 8.2). Other conditions were as described in the Materials and Methods section.

TABLE 1
Comparison of the Different Electron Acceptors With Respect to Power, Voltage, and Current Developed

Electron acceptor	PSI condition[a]	Maximum power output, μW[b]	Resistance at maximum power, Ω	Open circuit voltage, mV	Short Circuit current, mA	Short circuit current density, mA/cm^2	Maximum power conversion efficiency, %[c]
PMS	+	549	70	412	6.3	0.18	0.48
	−	484	70	397	5.9	0.17	—
PES	+	715	60	431	7.6	0.22	0.22[d]
	−	687	60	433	7.2	0.21	—
FMN[e]	+	2180	60	705	13.8	0.39	3.9
	−	1916	70	709	10.9	0.31	3.4
Photolyzed PMS	+	538	200	—	—	—	—
Photolyzed PES	+	548	200	—	—	—	—

+ Refers to filters containing active PSI particles.
− Refers to filters containing PSI particles inactivation with 15% TCA.
[b] Light intensity = 1970 W/m^2
[c] Light intensity = 39.3 W/m^2
[d] Light intensity = 19.7 W/m^2
[e] Sanderson et al. (9)

The PMS, PES, and FMN are known to undergo mechanistically complex photochemical reactions, producing a number of photoproducts. One of the major photoproducts of the relatively well studied PMS reaction is the 1-hydroxyl derivative of PMS, Py (Fig. 3) (*13,18–20*). Figure 4 is the cyclic voltammogram of a 0.5-m*M* anaerobic aqueous solution of PMS. Before photolysis, the redox couple corresponding to a reversible oxidation and reduction of PMS is located with a formal potential of −0.19 V vs SCE at pH 8.5. Upon photolysis, at least one new redox couple is generated with a midpoint potential, 0.18 V more negative than the PMS parent couple. Furthermore, upon continued photolysis, the current resulting from the PMS redox wave decreases with time, whereas that of the newly generated redox wave increases. This suggests a gradual conversion of PMS into another electrochemically active photoproduct. The new redox wave that arises from PMS photolysis is caused by the production of Py, since the cyclic voltammogram of isolated Py results in a similarly shaped reversible wave at the same formal potential (−0.37 V vs SCE) (not shown). Plots of the anodic peak potentials of PMS and Py vs pH (Fig. 5) show negative shifts in the redox potential with increasing pH. The slopes of the lines in Fig. 5 correspond to a two-electron redox reaction for PMS and a one-electron redox reaction for Py. The Py produced by photohydroxylation of PMS is quite stable in the basic, aqueous environment used in our solar cell and produces no electroactive photoproducts of its own.

Figure 6 is a cyclic voltammogram of an anaerobic aqueous solution of 0.5 m*M* PES, which shows a reversible redox wave with a formal potential of −0.16 V vs SCE at pH 8.0. Photolysis of the PES solution gives rise to a new, reversible redox wave, with a more negative formal potential than PES (−0.30 V vs SCE). Continued photolysis shows a gradual decrease in the current resulting from the PES redox couple and an increase in the current resulting from the formation of the electrochemically active photoproduct. The identity of this PES photoproduct is presumably the 1-hydroxyl derivative of PES. Plots of the anodic peak potentials of PES and PES-photoproduct are shown in Fig. 7. These plots show a negative shift in potential with increasing pH. The slopes of these

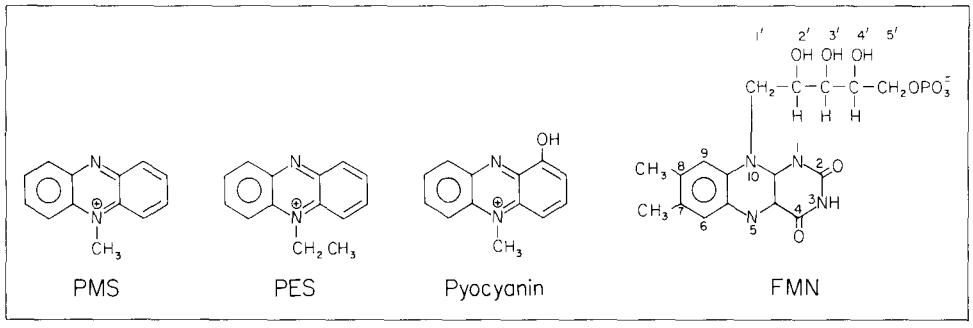

Fig. 3. Structures of PMS, PES, Py, and FMN.

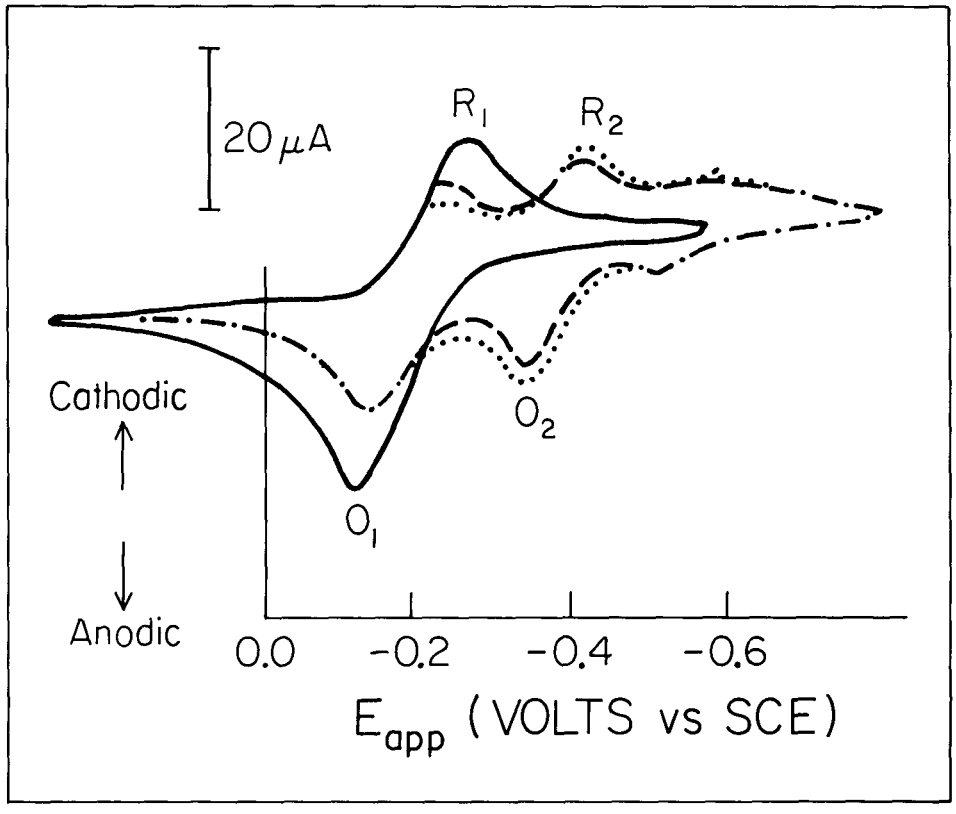

Fig. 4. Cyclic voltammogram of PMS before and after photolysis. The data were obtained under anaerobic conditions, using 0.5 m*M* PMS in 160 m*M* Tris-HCl (pH 8.5), at a carbon paste working electrode with a scan rate of 70 mV/s. (—), the cyclic voltammogram before photolysis; (-----), after 5 min of photolysis; (.....), after 15 min of photolysis. R_1/O_1 and R_2/O_2 correspond to the redox couples of PMS and Py, respectively. R and O represent the reduction and oxidation waves, respectively. The figure is plotted according to the polarographic convention. Other conditions were described in the Materials and Methods section.

lines correspond to a two-electron redox reaction for PES and a one-electron redox reaction for the photoproduct of PES.

These results imply that the power-producing species in the solar cell might not be PMS and PES as such, but, rather, their photoproducts. To test this hypothesis, PMS and PES were photolyzed prior to addition to the solar cell. In the case of photolyzed PMS (pyocyanin), the power developed was almost identical to that of the parent PMS (Table 1). Purified Py was also tested and gave comparable results. The power observed for photolyzed PES was 76% of the control. These data suggest that the active agent in power production in each case is the photolyzed product. This conclusion is in contrast to the work of Hisada et al. (*21*), who found that the photoproducts of PMS degradation were less effec-

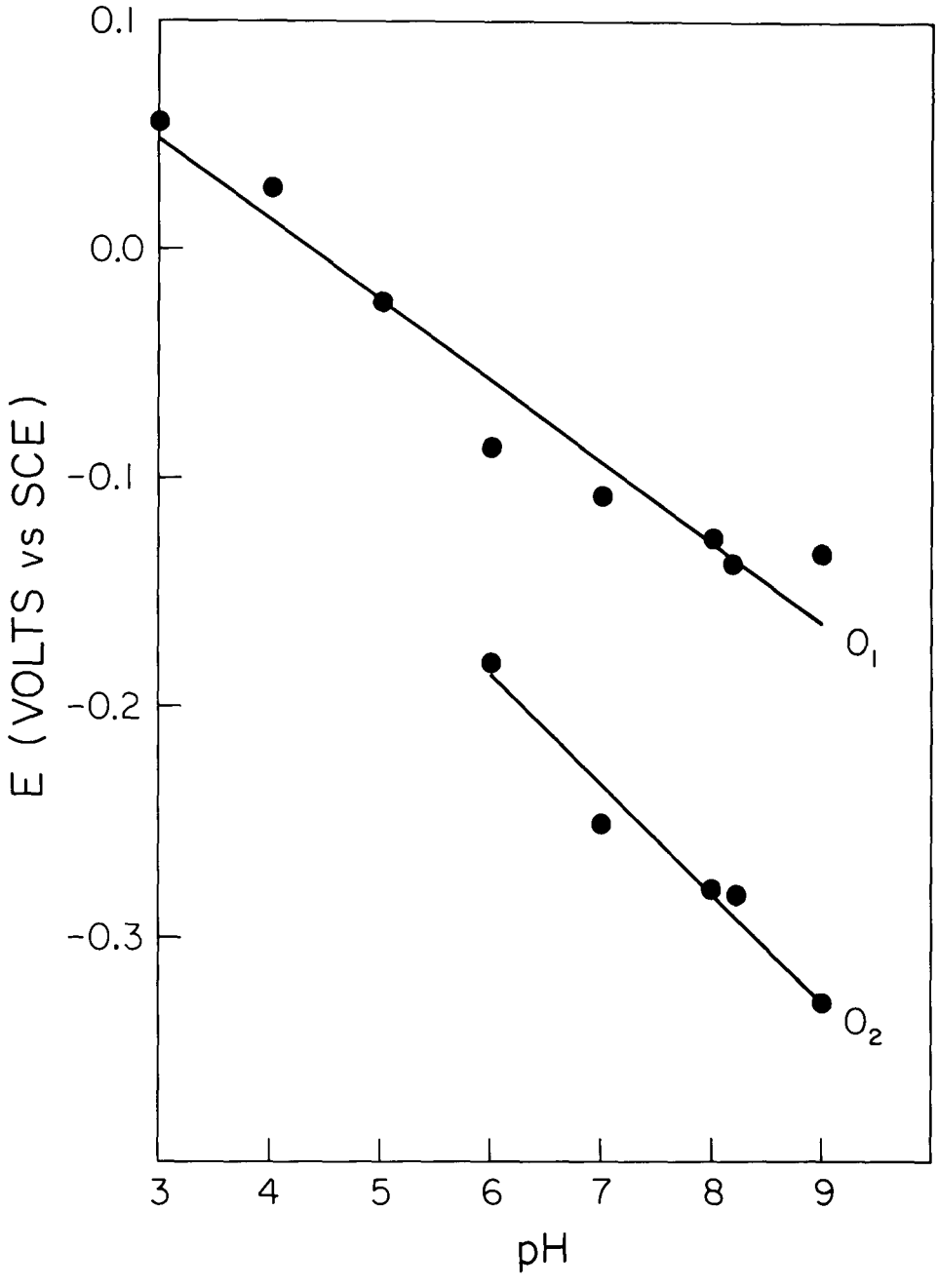

Fig. 5. Anodic peak potentials (E) for 0.5 mM PMS as a function of pH. Citrate/phosphate buffer was used in the 3–6 pH range. Tris-HCl buffer was used in the 7–9 pH range. Other conditions were as described for Figs. 2 and 4. The slope prior to photolysis, (O_1), corresponding to PMS, was 33.3 mV/pH unit, whereas that after photolysis, (O_2), corresponding to Py, was 55.4 mV/pH unit.

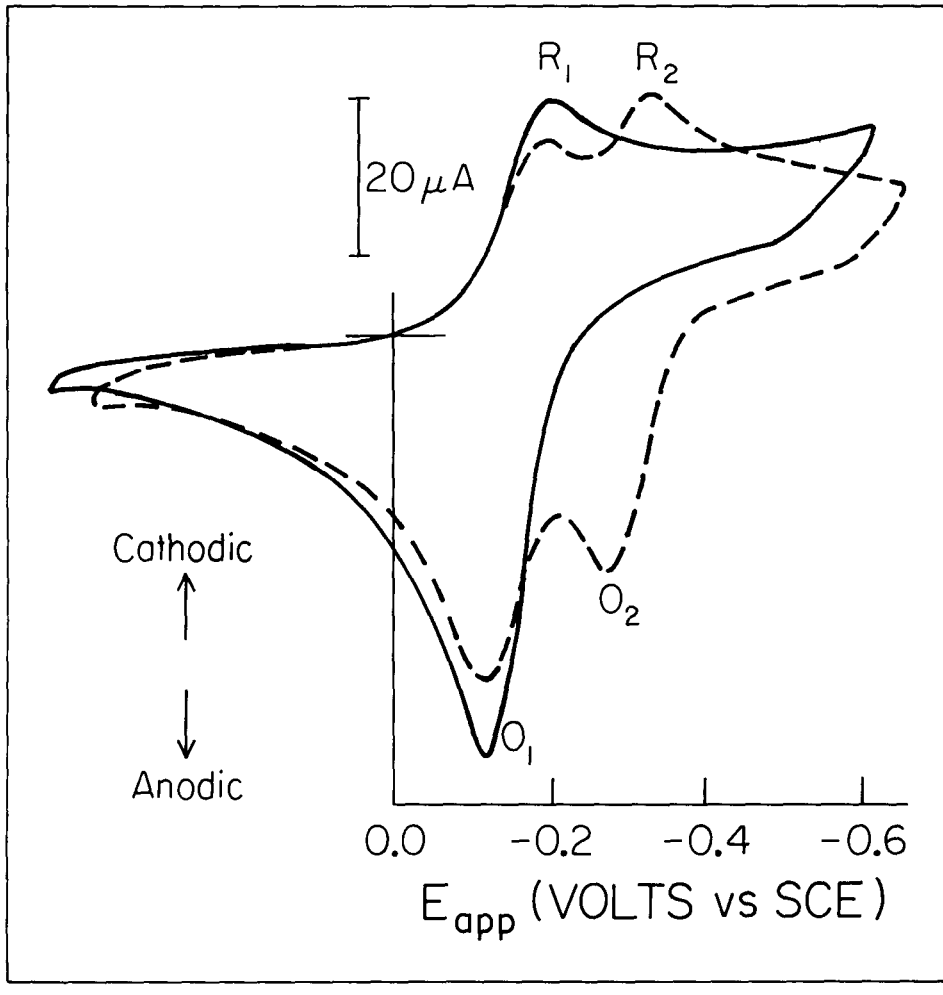

Fig. 6. Cyclic voltammogram of PES before and after photolysis. The data were obtained under anaerobic conditions, using 0.5 m*M* PES in 160 m*M* Tris-HCl (pH 8.0), at a carbon paste working electrode with a scan rate of 30 mV/s. The solid line (—) represents PES before photolysis and the dashed line (----) represents PES after 5 min of photolysis. R_1/O_1 and R_2/O_2 correspond to the redox couples of PES and the PES-photoproduct, respectively. Other conditions were as described for Fig. 4.

tive than the parent compound at mediating electron transport between NADH and nitrotetrazolium blue.

Our hypothesis is further supported by the results of a study on power output as a function of photolysis time, using PMS and PES as electron acceptors (Fig. 8). In both cases, power output increased rapidly over a 2-min photolysis time span to an intermediate plateau region that was maintained for approximately 2–3 more min. Immediately after this, however, a second increase in power output was observed. This second power surge rose gradually to the observed power maximum plateau and was maintained for at least 40 min of continuous illumination.

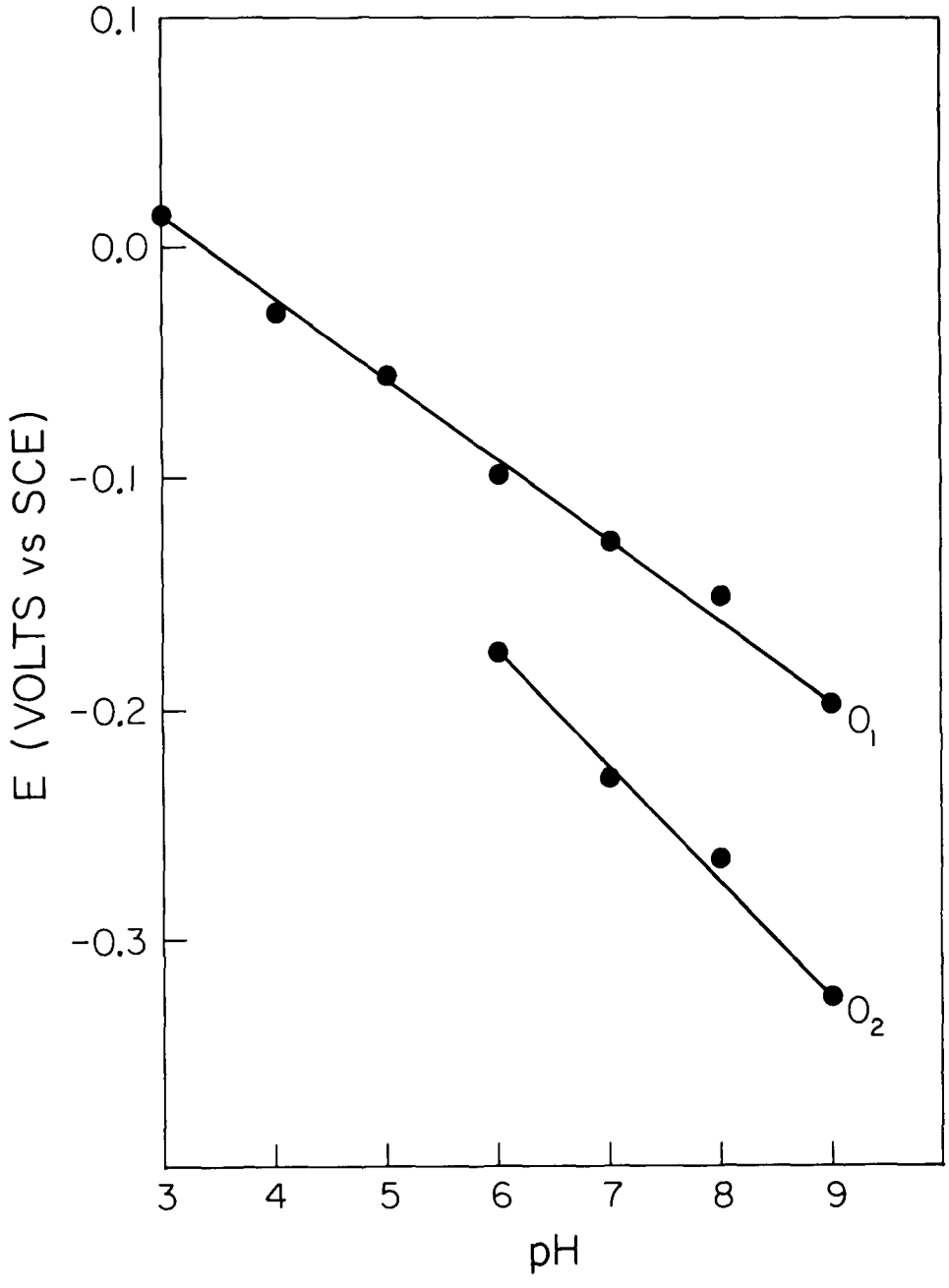

Fig. 7. Anodic peak potentials (E) for 0.5 mM PES as a function of pH. Conditions were the same as described for Fig. 5. O_1 and O_2 refer to PES solutions before and after photolysis. The slopes of the lines are as follows: O_1, 33.4 mV/pH unit; O_2, 50.3 mV/pH unit.

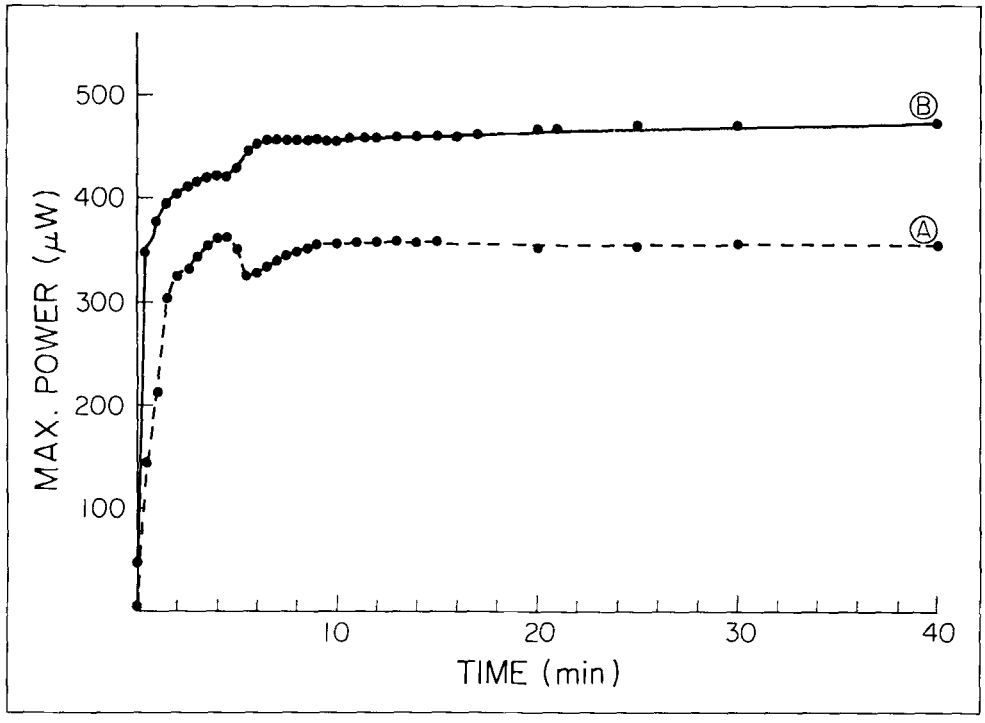

Fig. 8. Maximum power as a function of illumination time. Photovoltages were determined at different illumination times and the maximum power was calculated from these data. Other conditions were as described for Fig. 2. (A) (---), PMS; (B) (—), PES.

Figure 9 is a cyclic voltammogram of a 3-m*M* anaerobic aqueous solution of FMN that shows a reversible redox couple (A) with a formal potential of −0.48 V vs SCE at pH 8.0. Photolysis of the solution results in a complex assortment of electrochemically active photoproducts, with redox waves appearing more positive and more negative than the parent FMN redox couple. One of the major photoproducts of riboflavin (the precursor of FMN) is lumichrome (7,8-dimethylisalloxazine), which is known to be polarographically reduced at potentials more negative than that of riboflavin (*22*). Other photoproducts of riboflavin that have been identified as being formed under similar pH and ionic strength conditions used in our cell include 2′-ketoflavin 7,8-dimethyl-10-(1′-deoxy-D-erythro-2′-pentulosyl) isoalloxazine (*23,24*) and lumiflavin. The redox potential of this photoproduct is unknown. Other unidentified electrochemically active species may also represent the products of FMN photodestruction.

DISCUSSION

In contrast to other biological solar cells in which the photosynthetic component is immobilized directly on the electrode (*25–28*), the device in

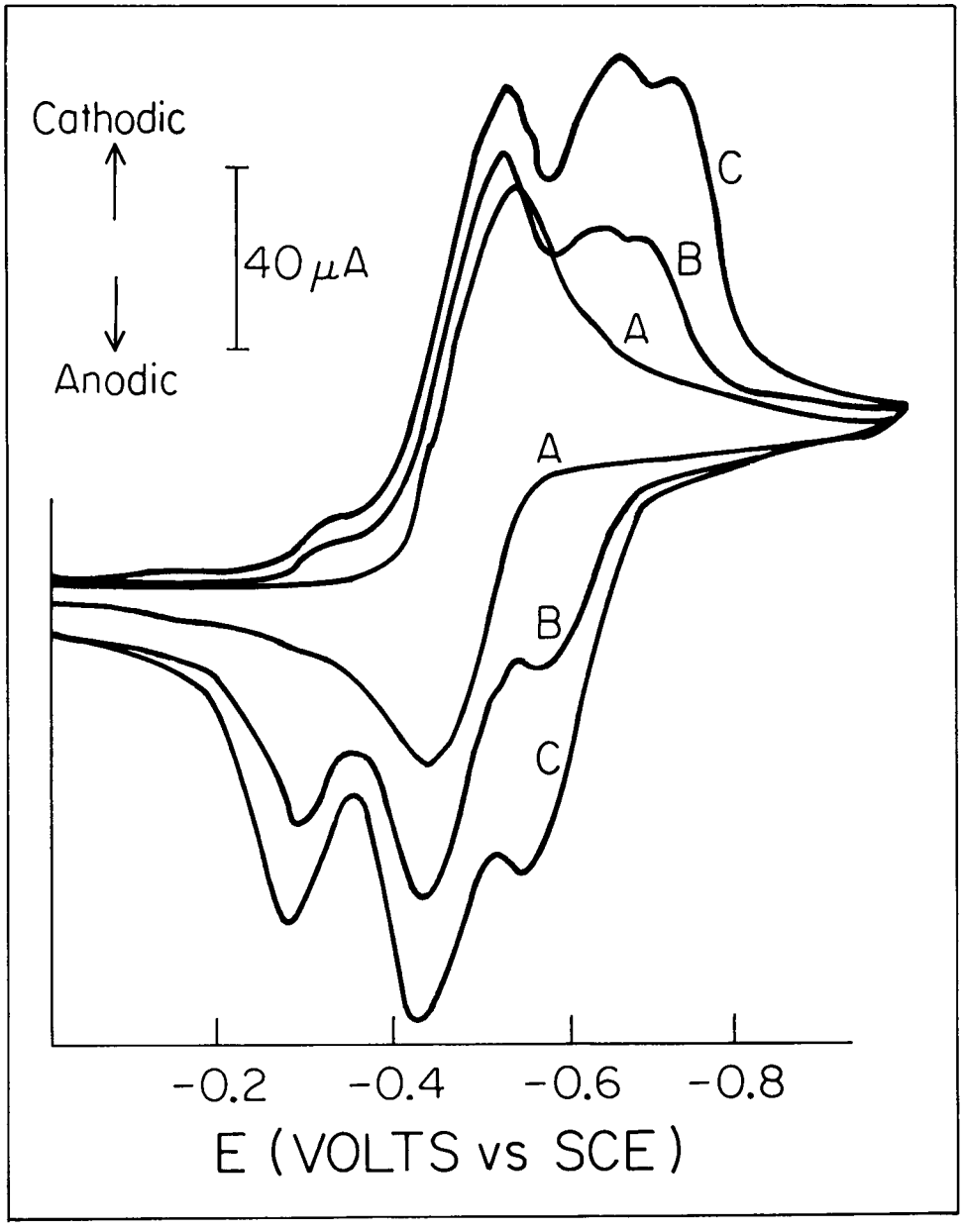

Fig. 9. Cyclic voltammogram of FMN before and after photolysis. The data were obtained under anaerobic conditions, using 3 m*M* FMN in 160 m*M* Tris-HCl (pH 8.0), at a carbon paste working electrode with a scan rate of 70 mV/s. (A) No photolysis; (B) 45 min of photolysis; and (C) 60 min of photolysis. Other conditions were as described in the Materials and Methods section.

this article uses the photosynthetic component (PSI) to separate the donor and acceptor half cells. The purpose of this study was to further characterize the exact mechanism of function in this type of cell.

The use of PMS, PES, and FMN with fairly positive formal potentials as electron acceptors from PSI resulted in unexpectedly good power outputs and conversion efficiencies compared to phenosafranin (*7*) or methyl viologen (*8*), which have lower redox potentials. A partial explanation for this anomalous behavior might lie in the observation that aqueous solutions of both PMS and PES produce electrochemically active photoproducts with formal potentials approximately 0.18 V more negative than the parent redox couple. Under conditions of continuous photolysis normally employed to operate the cell, parent PMS and PES molecules are converted to electrochemically active photoproducts very rapidly (Fig. 8). We suggest that the photoproducts can replace the parent compounds as electron acceptors in the cell. Since the photoproducts (Figs. 4 and 6) have more negative redox potentials than the parent compounds, a larger decrease in free energy potentially can be generated (Eq. 1). Hence, one observes a greater power output and conversion efficiency than would be expected. A similar phenomenon may also explain the results obtained for FMN.

Furthermore, PMS and its photoproduct Py, PES and its photoproduct, and FMN all exhibit negative shifts in redox potential with increasing pH. This observation explains why the cell operates more efficiently at pH 8.2 than at lower pH values (Fig. 2). The decrease in power observed at pH 8.5 may reflect a decrease in the photosynthetic contribution since PSI activity decreases at a pH greater than 8.

The PMS and PES, as well as FMN, contribute to both the photosynthetic and photochemical components of the solar cell output. The photosynthetic contribution appears much smaller (Table 1) in part because of the difference in active area illuminated. Note that the area of PSI particles illuminated was 1 cm^2 compared to 8 cm^2 for the electron acceptor. The two contributions appear more equal if maximum power output is compared on the basis of equal area illuminated. Using the data presented in Table 1, the photosynthetic contribution was calculated by subtracting the power observed with filters containing TCA-inactivated PSI from those with active PSI. The photochemical contribution was calculated by dividing the power obtained using inactivated PSI by 8 (i.e., 8 cm^2, the area of illumination). Table 2 shows that when compared in this manner, the photosynthetic and photochemical contributions are approximately equal. However, it should be noted that the photosynthetic contribution is smaller in the absence of a simultaneous photochemical contribution (*3,6*).

The $\Delta G^{\circ\prime}$ for the photosynthetic contribution (Eq. 2) can be calculated using Eq. (1) and is +117 kJ/mol using $K_4Fe(CN)_6$ as the electron donor and FMN as the electron acceptor. The $\Delta G^{\circ\prime}$ for the photochemical contribution can be estimated as outlined below. The products obtained from the anaerobic oxidation of EDTA include glyoxylate plus residual amine (*29*).

TABLE 2
Calculated Photosynthetic and Photochemical Contributions to the Maximum Power Output of the Photoelectrochemical Cell When Illuminated with Tungsten Light

Electron acceptor	Photosynthetic component, $\mu W/cm^2$	Photochemical component, $\mu W/cm^2$
PMS	65	61
PES	28	86
FMN	264	240

[a]Normalized to 1 cm^2 from the data in Table 1, as described in the text.

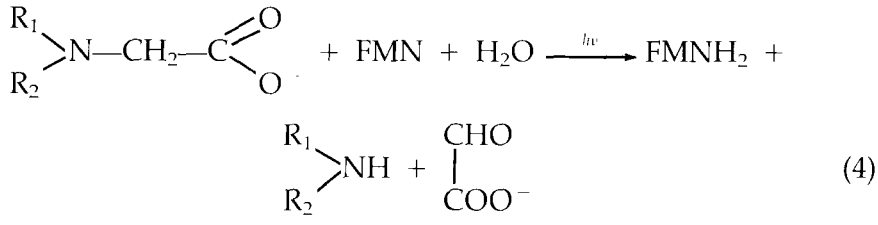

(4)

For computational purposes, this can be divided into two half-reactions:

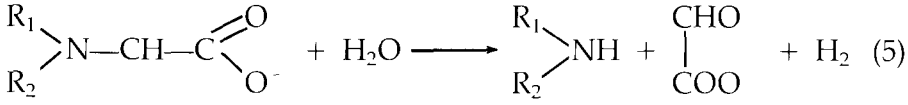

(5)

and:

(6)

Since the standard free energy of formation of EDTA is not available, the $\Delta G^{\circ\prime}$ for Eq. 5 was estimated using glycine as a substitute for EDTA.

(7)

Taking the standard free energy of formation of glycine from the *Handbook of Biochemistry and Molecular Biology* (*30*) and the values for the other reactants and products from National Bureau of Standards (NBS) circular 500 (*31*), we calculated a $\Delta G^{\circ\prime}$ of +62.7 kJ/mol for the Eq. 7 half-reaction. The $\Delta G^{\circ\prime}$ for the reduction of FMN by H_2 at pH 7 (Eq. 6) is −44.3 kJ/mol. Combining these two half reactions yields an estimated $\Delta G^{\circ\prime}$ of +18.4 kJ/mol for the total reaction of Eq. 4 in the absence of light input. The actual Gibbs free energy change of a reaction at pH 7 ($\Delta G'$) will, of course, depend on the ratio of products to reactants under steady-state conditions. In the light, Eq. 4 proceeds to the right. One can calculate the maximum rate of EDTA oxidation under conditions of maximum power output (1916 μW from an illuminated area of 8 cm^2, Table 1) and from that rate derive an equation that relates the power output of the cell to the $\Delta G'$ of the light-driven reaction. The result of the calculation gives a $\Delta G'$ of −70.2 kJ/mol. The difference between this value and the above-estimated $\Delta G^{\circ\prime}$ for the reaction in the absence of light is an indication of the energy light contributes to the photochemical reaction in the cell.

Nevertheless, thermodynamically, much more energy is potentially stored by the photosynthetic than the photochemcial reaction. The fact that we observe approximately an equal contribution of the two reactions to the power output of the cell tells us that kinetic factors involved in the photosynthetic reaction are suboptimal compared to those involved in the photochemical reaction.

There are two possible directions for future research. One would emphasize improvement of the photochemical contribution. This would eliminate the need to isolate and stabilize the PSI particles. On the other hand, it would be necessary to surmount the sacrificial nature of the photochemical contribution (i.e., regenerate $EDTA_{red}$ or equivalent in Fig. 1), which is currently nonreversible. The second approach is to improve the photosynthetic contribution and make it independent of the photochemical contribution. The advantages of this approach are that the reaction center of the PSI particles (which converts the light energy to chemical potential) is cyclic in nature, and the antenna chlorophyll molecules in the complex are arranged for efficient absorption of light energy (*4,32*). To do this, however, one must redesign the cell so as to allow optimal illumination of the PSI particles, enhance the activity and lifetime of the PSI particles, and find nonphotochemically active redox agents to couple the oxidizing and reducing side of PSI to their respective electrodes.

ACKNOWLEDGMENTS

This work was supported in part by US Department of Energy Grants #DE-FG02-79ER10538 (ELG) and FTP-18-006-86 (MS). Any opinions, findings, or conclusions expressed herein do not necessarily reflect the views of DOE.

REFERENCES

1. Bhardwaj, R., Pan, R. L., and Gross, E. L. (1981), *Nature* **289,** 369.
2. Bhardwaj, R., Pan, R. L., and Gross, E. L. (1981), *Proc. Ann. Meet. Am. Sec. Intl. Solar Energy Soc.* **4.1,** 184.
3. Bhardwaj, R., Pan, R. L., and Gross, E. L. (1981), in *Proc. Fifth Intl. Photosynth. Congr.*, **6,** Akoyunoglou, G., ed. Balaban International Science Services, Philadelphia, PA, pp. 719–728.
4. Wraight, C. A. (1982), in *Photosynthesis: Energy Conversion by Plants and Bacteria*, **I,** Govindjee, ed., Academic, NY, NY, p. 17.
5. Gross, E. L., Youngman, D. R., and Winemiller, S. L. (1978), *Photochem. Photobiol.* **28,** 249.
6. Pan, R. L., Bhardwaj, R., and Gross, E. L. (1982), *Photochem. Photobiol.* **35,** 655.
7. Bhardwaj, R., Pan, R. L., and Gross, E. L. (1981), *Photochem. Photobiol.* **34,** 215.
8. Bhardwaj, R., Pan, R. L., and Gross, E. L. (1981), *Photobiochem. Photobiophys.* **3,** 19.
9. Sanderson, D. G., Pan, R. L., and Gross, E. L. (1983), *App. Biochem. Biotech.* **8,** 395.
10. Shiozawa, J. A., Alberte, R. S., and Thornber, J. P. (1974), *Arch. Biochem. Biophys.* **165,** 388.
11. Gross, E. L., and Grenier, J. (1978), *Arch. Biochem. Biophys.* **187,** 387.
12. Arnon, D. I. (1949), *Plant Physiol.* **24,** 1.

13. McIlwain, H. (1937), *J. Chem. Soc.* **2,** 1704.
14. Knight, M., Hartman, P. E., Hartman, Z., and Young, V. M. (1979), *Anal. Biochem.* **95,** 19.
15. Baron, S. S., and Rowe, J. J. (1981), *Antimicrob. Agents Chemother.* **20,** 814.
16. Blackwood, A. C., and Neish, A. D. (1957), *Can. J. Microbiol.* **3,** 165.
17. Ingledew, W. M., and Campbell, J. J. R. (1969), *Can. J. Microbiol.* **15,** 535.
18. Chew, V. S. F., and Bolton, J. R. (1980), *J. Phys. Chem.* **84,** 1903.
19. Chew, V. S. F., and Bolton, J. R. (1980), *J. Phys. Chem.* **84,** 1909.
20. Morrison, M. M., Seo, E. T., Howie, J. K., and Sower, D. T. (1978), *J. Am. Chem. Soc.* **100,** 207.
21. Hisada, R., Shinkai, W., and Yagi, T. (1981) *J. Appl. Biochem.* **3,** 535.
22. Brdicka, R., and Knoblock, E. (1941), *Z. Elektrochem.* **47,** 721.
23. Treadwell, G. E., Cairns, W. L., and Metzler, D. E. (1968), *J. Chromatog.* **35,** 376.
24. Cairns, W. L., and Metzler, D. E. (1971), *J. Am. Chem. Soc.* **93,** 2772.
25. Janzen, A. F., and Seibert, M. (1980) *Nature* **286,** 584.
26. Ochiai, H., Shibata, H., Sawa, Y., and Katoh, T. (1980), *Proc. Natl. Acad. Sci. USA* **77,** 2442.
27. Seibert, M., and Kendall-Tobias, M. W. (1982), *Biochim. Biophys. Acta* **681,** 504.
28. Seibert, M., Janzen, A. F., and Kendall-Tobias, M. W. (1982), *Photochem. Photobiol.* **35,** 193.
29. Enns, K., and Burgess, W. H. (1965), *J. Am. Chem. Soc.* **87,** 5766.
30. Hutchens, J. O. (1976), in *Handbook of Biochemistry and Molecular Biology,* 3rd edition, **I,** Fasman, G.D., ed., CRC, Cleveland, OH, p. 118.
31. Rossini, F. D., Wagman, D. D., Evans, W. H., Levine, S., and Jaffe, I. (1952), *Selected Values of Chemical Thermodynamic Properties,* NBS Circular 500.
32. Kaplan, S., and Arntzen, C. J. (1982), in *Photosynthesis: Energy Conversion by Plants and Bacteria,* **I,** Govindjee, ed., p. 67.